J. Phys. B: At. Mol. Phys. **14** (1981) 2429–2448. Printed in Great Britain

A third-order optical potential theory for elastic scattering of electrons and positrons by atomic hydrogen

F W Byron Jr† and C J Joachain‡§

† Department of Physics and Astronomy, University of Massachusetts, Amherst, Massachusetts 01003

‡ Physique Théorique, Faculté des Sciences, Université Libre de Bruxelles, Brussels, Belgium

§ Institute de Physique Corpusculaire, Université de Louvain, Louvain-la-Neuve, Belgium

Received 29 September 1980, in final form 17 February 1981

Abstract. We analyse the elastic scattering of electrons and positrons by atomic hydrogen at intermediate energies (50–500 eV) by using the basic ideas of the eikonal–Born series method to construct from first principles a local third-order optical potential. In addition to the first-order (static) interaction, our optical potential contains a complex second-order part, obtained from improved values of the second Born approximation to the scattering amplitude, and also the leading contribution of the third-order part. Exchange effects are taken into account by means of a local pseudopotential. A full wave treatment of the optical potential is then performed, and a detailed comparison is made with recent absolute measurements of e^-–H differential cross sections. Total (integrated) elastic and total (complete) cross sections for both electron and positron impact are also discussed.

1. Introduction

Among the theoretical methods which have been successfully applied in recent years to analyse the elastic scattering of fast electrons and positrons by atoms (Bransden and McDowell 1977, 1978, Byron and Joachain 1977a), the optical potential approach has attracted considerable interest. Nearly all the *ab-initio* calculations of the optical potential done so far have been performed by expanding it through *second order* in the interaction between the projectile and the target. In particular, our previous optical-model study of the elastic scattering of fast electrons and positrons by complex atoms (Byron and Joachain 1974a, 1977b (to be referred to as I), Joachain *et al* 1977) consisted of constructing from first principles a local, energy-dependent, second-order optical potential. In addition to the first-order (static) interaction, this potential contained a complex second-order contribution whose real part accounts for dynamic polarisation effects, while the imaginary part represents the loss of flux from the incident channel. For incident electrons our optical potential also included a pseudopotential which takes into account exchange effects. A full wave treatment of this second-order optical potential was then carried out. The resulting theory is thus a unitarisation of the lowest orders of perturbation theory. This unitarisation is particularly important at large angles where the inclusion of the singular electron (positron)–

0022-3700/81/142429+20$01.50

nucleus Coulomb interaction to all orders of perturbation theory has a significant effect (Byron and Joachain 1977a, b).

In the course of constructing our second-order optical potential, the basic ideas of the eikonal–Born series (EBS) approximation (Byron and Joachain 1973, 1977a, 1977c to be referred to as II), were used extensively. In the present paper we shall again use the EBS method to construct a local, *third-order* optical potential, which will be used to study the elastic scattering of fast electrons and positrons by atomic hydrogen. Since the target eigenfunctions are known exactly in this case, it is worthwhile to refine the dynamical description of the scattering process. Accordingly, we have not only added to our optical potential the leading contribution from the third-order part, but we have also increased the accuracy of the second-order contribution by using improved values for the second Born approximation to the scattering amplitude.

We begin in § 2 by discussing the evaluation of our optical potential, with particular emphasis on the new aspects of our calculations concerning the second-order contribution and on the determination of the third-order part. Section 3 is devoted to the application of our optical potential to the elastic scattering of electrons and positrons by atomic hydrogen, in the energy range between 50 and 500 eV. A detailed comparison of our differential cross sections is made with EBS results and with recent absolute experimental data (Lloyd *et al* 1974, Williams 1975, van Wingerden *et al* 1977) obtained for incident electrons. Our total (integrated) elastic and total (complete) cross sections, obtained for both electron and positron impact, are also compared with other theoretical calculations (Winters *et al* 1974, Vanderpoorten 1975, Winick and Reinhardt 1978). A comparison is also made with experimental values of total elastic cross sections for e^-–H scattering, obtained recently by Williams (1975) and van Wingerden *et al* (1977).

2. Calculation of the optical potential

In this section we shall follow the conventions of papers I and II. In particular, scattering wavefunctions are normalised so that $\langle \boldsymbol{q} | \boldsymbol{q}' \rangle = \delta(\boldsymbol{q} - \boldsymbol{q}')$ and bound state eigenkets of the hydrogen Hamiltonian will be denoted by $|n\rangle$ and their eigenvalues by w_n. The initial and final momenta of the electron or positron are denoted respectively by $\boldsymbol{k}_i$ and $\boldsymbol{k}_f$, with $k = |\boldsymbol{k}_i| = |\boldsymbol{k}_f|$. The momentum transfer is $\boldsymbol{K} = \boldsymbol{k}_i - \boldsymbol{k}_f$.

2.1. The first-order optical potential

As discussed in I, the lowest order contribution to the optical potential is just the full electron(positron)–atom potential averaged over the ground state of the atom. Thus, we have for the first-order optical potential

$$V^{(1)}(r) = Q\left\langle 1\mathrm{s}\left|\frac{1}{r} - \frac{1}{|\boldsymbol{r} - \boldsymbol{r}_1|}\right|1\mathrm{s}\right\rangle \tag{1}$$

where $\boldsymbol{r}_1$ denotes the coordinate of the 1s electron in the target, $Q = -1$ for incident electrons and $Q = +1$ for incident positrons. Equation (1) is easily evaluated, and yields the static potential

$$V^{(1)}(r) = Q\left(1 + \frac{1}{r}\right)\mathrm{e}^{-2r} = V_{\mathrm{st}}(r). \tag{2}$$

2.2. The second-order optical potential

Since the second term in the Born series can be readily evaluated in closed form by use of the closure approximation, it would be a simple matter to construct a second-order contribution to the optical potential based on this approximation. Of course, since the optical potential has V_{st} as its lowest order part, we would be counting the intermediate 1s state twice unless we subtracted this state from the second Born term. However, in the case of atomic hydrogen, for which the wavefunctions are known exactly, it seems worthwhile to see if we can improve somewhat on the above proposal.

First of all, as we have remarked elsewhere, it makes good sense to include the ground state exactly in our approximate second Born term, since this will guarantee that the large momentum transfer behaviour of the amplitude will be given correctly. Furthermore, since the 2p state contributes in such an important way to the polarisation sum rule, we expect that it will make a significant contribution to the real part of the second Born term. For this reason, we shall also include the 2s and 2p states exactly in our approximate second Born amplitude.

Rather than undertake the tedious task of including more and more target states exactly, it seems reasonable at this point to sum the remaining states by the use of the closure approximation. This immediately raises the question of how to determine $\bar{w}$, the average excitation energy of the closure method, in an optimal manner. In earlier papers, we chose $\bar{w}$ to give the correct value of Im $\bar{f}_{B2}(K=0)$ at high energy (400 eV for e^-+H scattering), which led to a value $\bar{w}=0.465$ au. However, it is by no means obvious that the same choice will be satisfactory for Re $\bar{f}_{B2}$. Fortunately, the evaluation of Re $\bar{f}_{B2}(K=0)$, although not as simple as the evaluation of Im $\bar{f}_{B2}(K=0)$, is relatively straightforward to carry out. In fact, Holt (1972) evaluated $\bar{f}_{B2}(K=0)$ for various values of k, and we have verified his results independently using a different calculational procedure. Details of this procedure are given in the appendix. We have therefore attempted to determine an average excitation energy, $\bar{w}_R$, for the real part of the approximate second Born term by requiring that $\bar{w}_R$ should give the correct value of Re $f_{B2}(K=0)$ at a given value of k, which we choose to be $k=4$. Unfortunately, we discovered that there is no value of $\bar{w}_R$ which satisfies this criterion.

The reason for this unexpected result may be seen by examining in detail the contributions to the forward second Born amplitude coming from the individual intermediate states of different angular momentum. One finds that in the bound-state region the $l=1$ intermediate states have a very different behaviour as a function of the intermediate-state energy than do the states with $l\neq 1$.

Figure 1 shows the contribution of the $l=1$ intermediate states with $n>2$ to Re $\bar{f}_{B2}(K=0)$ as a function of the intermediate-state energy. In the discrete part of the spectrum the contributions have been multiplied by n^3 so they will join smoothly onto the continuous part of the spectrum. In displaying the $l=1$ results we have omitted the contribution of order k^{-1} which comes from the polarisability of the atom, since in practice this contribution (which is equal to π/k and is independent of the average excitation energy) can always be included exactly in Re $\bar{f}_{B2}$ in the small-angle region where it is important. This k^{-1} part is unique to $l=1$ states, so by omitting it we are able to give a meaningful comparison with states having $l\neq 1$. Figure 2 is similar to figure 1 but shows the contributions of $l=2$ intermediate states. The contrast between the two figures is striking, the $l=1$ contributions always being negative in the bound state region and the $l=2$ contributions always being positive, as are those of all other $l\neq 1$. As one varies the excitation energy off-shell, the p states contribute to the sum over states in a very different way from all the other states.

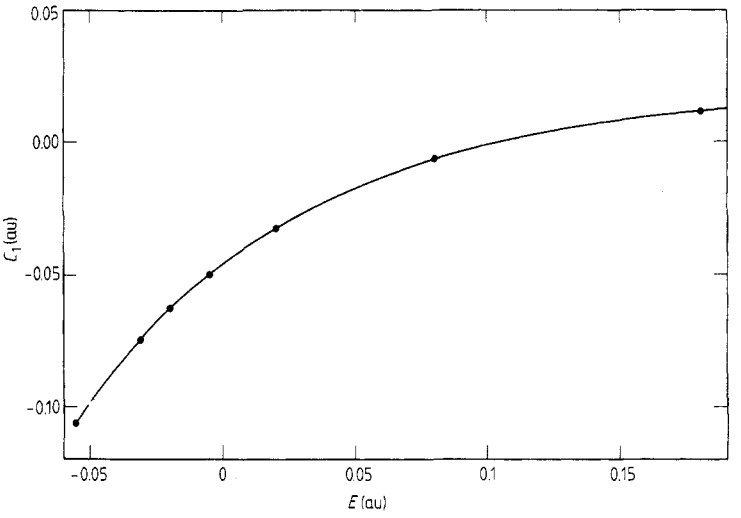

Figure 1. The contribution C_1 of the $l = 1$ intermediate states with $n > 2$ to Re $\bar{f}_{B2}(K = 0)$, as a function of the intermediate state energy. The part of order k^{-1} arising from the polarisability of the atom has been removed, and the contributions coming from the discrete part of the spectrum have been multiplied by n^3.

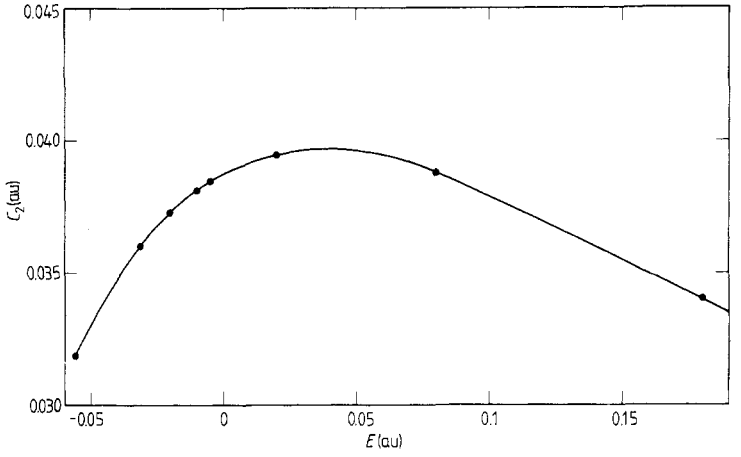

Figure 2. The contribution C_2 of the $l = 2$ intermediate states with $n > 2$ to Re $\bar{f}_{B2}(K = 0)$, as a function of the intermediate state energy. The contributions coming from the discrete part of the spectrum have been multiplied by n^3.

Given this situation, an obvious approach is to create, in a manner similar to Damburg and Karule (1967), an $l = 1$ pseudostate, $|3\bar{p}\rangle$, orthogonal to $|2p\rangle$, which duplicates the contribution of the bound p states with $n > 2$. This is easily done, and one finds

$$\langle \boldsymbol{r} | 3\bar{p}\rangle = 0.24648r(1 - 0.1822r) \exp(-0.411r) Y_{1m}(\theta, \phi). \tag{3}$$

For this state, the average value of the atomic Hamiltonian is $w_{3\bar{p}} = -0.050$ au, so the pseudostate is 'bound'. With this state obtained, we now may re-evaluate the real part of the forward amplitude with the states 1s, 2s, 2p and $3\bar{p}$ included exactly and again

account for the remaining states by closure. Varying $\bar{w}_R$ to obtain the correct value for Re $\bar{f}_{B2}(K=0)$ at $k=4$, one finds $\bar{w}_R = 1.61$ au, i.e., the average excitation energy of the remaining states lies a bit more that 1 au into the continuum. Such a large excitation energy may at first seem surprising, but in evaluating Re $\bar{f}_{B2}(K=0)$ one finds that with the 1s, 2s, 2p and 3p̄ states included 96% of the remaining contributions come from the continuum and that rather high values of l are important (states with $l>2$ contribute 30%). Thus, an excitation energy located well into the continuum is by no means unreasonable.

We may add parenthetically that the situation described above is rather special to elastic scattering. We have made a similar calculation of Re $\bar{f}_{B2}(K=0)$ for the 1s–2s excitation of atomic hydrogen, and here one finds that with the states 1s, 2s and 2p included, the remaining contribution is strongly dominated by the other $l=1$ states, with the continuum playing a rather minor role. The value $\bar{w}_R = 0.44$ au then yields a closure result in precise agreement with the exact result at $k=4$. It is also worth noting that exact second Born calculations have been performed recently over the full angular range for elastic e^-–H scattering at 30 eV (Ermolaev and Walters 1979) and for 1s–2s excitation of atomic hydrogen at 54.4 eV (Ermolaev and Walters 1980).

Let us now summarise the situation for elastic scattering. For the imaginary part of $\bar{f}_{B2}$ we use the procedure of II in which the ground state is included exactly and an average excitation energy $\bar{w}_I = 0.465$ au is used to carry out the remaining sum on intermediate states. For the real part of $\bar{f}_{B2}$, we include the 1s, 2s, 2p and 3p̄ states exactly and use an average excitation energy $\bar{w}_R = 1.61$ au to carry out the remaining sum on intermediate states. In addition, for both real and imaginary parts, we treat, respectively, the terms of order k^{-1} and $k^{-1}\ln k$ at small angles in the manner described in II. Denoting the resulting real and imaginary parts of $\bar{f}_{B2}$ by $f_{B2R}^{\bar{w}_R}$ and $f_{B2I}^{\bar{w}_I}$, we then write

$$\bar{f}_{B2} \simeq f_{B2R}^{\bar{w}_R} + i f_{B2I}^{\bar{w}_I}. \tag{4}$$

Table 1 shows the values obtained in this way for $\bar{f}_{B2}$, in the case of elastic electron–atomic-hydrogen scattering at 100 and 200 eV.

With $\bar{f}_{B2}$ approximated in this manner, we remove the 1s state to form the quantity

$$\bar{f}_{B2,Opt} = \bar{f}_{B2} - 8\pi^2 \int \frac{\langle \boldsymbol{k}_f | V_{st} | \boldsymbol{q} \rangle \langle \boldsymbol{q} | V_{st} | \boldsymbol{k}_i \rangle}{q^2 - k^2 - i\varepsilon} \, d\boldsymbol{q} \qquad \varepsilon \to 0^+ \tag{5}$$

and then obtain a local, central second-order optical potential $V^{(2)}(r)$ by requiring that

$$\bar{f}_{B2,Opt}(K) = -\frac{1}{2\pi} \int \exp(i\boldsymbol{K}\cdot\boldsymbol{r}) V^{(2)}(r) \, d\boldsymbol{r}. \tag{6}$$

Using the Fourier integral theorem, we have from equation (6)

$$\begin{aligned} V^{(2)}(r) &= -\frac{1}{4\pi^2} \int \exp(-i\boldsymbol{K}\cdot\boldsymbol{r}) \bar{f}_{B2,Opt}(K) \, d\boldsymbol{K} \\ &= -\frac{1}{\pi r} \int_0^\infty K \sin Kr \, \bar{f}_{B2,Opt}(K) \, dK. \end{aligned} \tag{7}$$

Clearly, $V^{(2)}(r)$ will be energy dependent and will have both a real and an imaginary part:

$$V^{(2)}(r) = V_R^{(2)}(r) + i V_I^{(2)}(r). \tag{8}$$

We shall refer to $V_I^{(2)}$ as the absorption potential.

Table 1. Values of the second Born term $\bar{f}_{B2}$, corresponding to the elastic scattering of electrons by atomic hydrogen at 100 and 200 eV, as obtained by the present calculations. The numbers in parentheses indicate powers of 10.

θ (deg)	$E = 100$ eV		$E = 200$ eV	
	$f_{B2}^{\bar{w}R}$	$f_{B2}^{\bar{w}I}$	$f_{B2}^{\bar{w}R}$	$f_{B2}^{\bar{w}I}$
0	1.35	1.58	9.21 (−1)	1.32
5	6.57 (−1)	1.31	2.37 (−1)	8.36 (−1)
10	3.47 (−1)	9.06 (−1)	1.00 (−1)	4.63 (−1)
15	2.09 (−1)	6.14 (−1)	5.53 (−2)	2.84 (−1)
20	1.38 (−1)	4.31 (−1)	3.67 (−2)	1.98 (−1)
25	9.74 (−2)	3.21 (−1)	2.78 (−2)	1.55 (−1)
30	7.37 (−2)	2.55 (−1)	2.27 (−2)	1.32 (−1)
35	5.91 (−2)	2.16 (−1)	1.92 (−2)	1.17 (−1)
40	4.96 (−2)	1.91 (−1)	1.65 (−2)	1.06 (−1)
50	3.79 (−2)	1.61 (−1)	1.24 (−2)	8.86 (−2)
60	3.07 (−2)	1.42 (−1)	9.49 (−3)	7.55 (−2)
70	2.57 (−2)	1.27 (−1)	7.45 (−3)	6.53 (−2)
80	2.18 (−2)	1.16 (−1)	6.01 (−3)	5.73 (−2)
90	1.88 (−2)	1.06 (−1)	4.99 (−3)	5.10 (−2)
100	1.65 (−2)	9.74 (−2)	4.25 (−3)	4.61 (−2)
120	1.33 (−2)	8.52 (−2)	3.31 (−3)	3.92 (−2)
140	1.14 (−2)	7.74 (−2)	2.80 (−3)	3.50 (−2)
160	1.04 (−2)	7.32 (−2)	2.54 (−3)	3.28 (−2)
180	1.01 (−2)	7.18 (−2)	2.46 (−3)	3.21 (−2)

2.3. The third-order optical potential

We shall now obtain the third-order optical potential $V^{(3)}$ by a simple extension of the method which was used in I to generate the absorption potential. Using a notation similar to that of I, we write the optical eikonal amplitude (Byron and Joachain 1974b) as

$$f_{OE} = \frac{k}{2\pi i}\int \exp(i\boldsymbol{K}\cdot\boldsymbol{b})\{\exp[(i/k)(V_0\chi_1 + iV_0^2\chi_2 + V_0^3\chi_3)] - 1\}\,d^2b \qquad (9)$$

where

$$V_0^n\chi_n = -\int_{-\infty}^{\infty} V_n(\boldsymbol{b}, z)\,dz \qquad n = 1, 2, 3 \qquad (10)$$

and we have used V_0 to denote a coupling constant for this problem, which we shall later set equal to unity. In addition to the terms already present in I, we have added a third-order phase function, χ_3, which we assume to be derivable from a local potential, V_3. On the other hand, the many-body Glauber amplitude may be written as

$$f_G = \frac{k}{2\pi i}\int \exp(i\boldsymbol{K}\cdot\boldsymbol{b})\langle 1s|\exp[(i/k)V_0\hat{\chi}_G(\boldsymbol{b}-\boldsymbol{b}_1)] - 1|1s\rangle\,d^2b \qquad (11)$$

where $\hat{\chi}_G$ is the familiar Glauber phase,

$$\hat{\chi}_G = -Q\ln[(\boldsymbol{b}-\boldsymbol{b}_1)^2/b^2] \qquad (12)$$

with $\boldsymbol{b}$ denoting the impact parameter of the incident electron and $\boldsymbol{b}_1$ that of the bound electron.

Expanding equation (9) in powers of V_0 and keeping all terms through order V_0^3, we have

$$f_{OE}=\frac{1}{2\pi}\int \exp(i\boldsymbol{K}\cdot\boldsymbol{b})\Big(V_0\chi_1+iV_0^2\chi_2+V_0^3\chi_3+\frac{i}{2k}(V_0^2\chi_1^2+2iV_0^3\chi_1\chi_2)$$

$$-\frac{1}{6k^2}V_0^3\chi_1^3+\ldots\Big)\,d^2b. \tag{13}$$

A similar expansion of f_G gives

$$f_G=\frac{1}{2\pi}\int \exp(i\boldsymbol{K}\cdot\boldsymbol{b})\Big(V_0\langle 1s|\hat{\chi}_G|1s\rangle+\frac{i}{2k}V_0^2\langle 1s|\hat{\chi}_G^2|1s\rangle-\frac{1}{6k^2}V_0^3\langle 1s|\hat{\chi}_G^3|1s\rangle+\ldots\Big)\,d^2b. \tag{14}$$

Equating equal powers of V_0 we obtain readily

$$\chi_1^G=\langle 1s|\hat{\chi}_G|1s\rangle \tag{15a}$$

$$\chi_2^G=\frac{1}{2k}(\langle 1s|\hat{\chi}_G^2|1s\rangle-\langle 1s|\hat{\chi}_G|1s\rangle^2) \tag{15b}$$

$$\chi_3^G=-\frac{1}{6k^2}(\langle 1s|\hat{\chi}_G^3|1s\rangle-3\langle 1s|\hat{\chi}_G^2|1s\rangle\langle 1s|\hat{\chi}_G|1s\rangle+2\langle 1s|\hat{\chi}_G|1s\rangle^3) \tag{15c}$$

where we add a superscript G to χ_n to indicate that χ_n is obtained in the Glauber approximation. With $\chi_n^G(k,r)$ determined in this way, equation (10) may be inverted to obtain

$$V_n^G(k,r)=\frac{1}{\pi}\int_r^\infty (b^2-r^2)^{1/2}\frac{d}{db}\chi_n^G(k,b)\,db. \tag{16}$$

For V_1^G one can actually evaluate equation (16) in closed form. One obtains

$$V_1^G(k,r)=Q\Big(1+\frac{1}{r}\Big)\exp(-2r) \tag{17}$$

which is just the familiar static potential of equation (1). The potentials V_2^G and V_3^G must be obtained numerically from equations (15*b*), (15*c*) and (16). We may clearly write, according to equations (15*b*) and (15*c*)

$$V_2^G(k,r)=k^{-1}v_2^G(r) \tag{18a}$$

$$V_3^G(k,r)=k^{-2}v_3^G(r) \tag{18b}$$

where v_n^G is independent of k. The functions v_2^G and v_3^G are plotted in figure 3. In plotting v_3^G, we have set $Q=-1$, so this is the function appropriate to electron–hydrogen scattering. The function v_2^G is independent of Q, since for both electrons and positrons, $Q^2=1$. It is worth noting that at large r the asymptotic forms of the functions v_2^G and v_3^G are given by $v_2^G\simeq -1/r^3$ and $v_3^G(r)\simeq 9Q/2r^5$, respectively.

In what follows we shall use V_3^G as the third-order term $V^{(3)}$ of our optical potential. It seems very likely that it gives the leading contribution (of order k^{-2}) to the third Born term so that with V_3^G included in our optical potential we have an expression for the direct part of V_{opt} correct through order k^{-2}. The function $V_2^G(k,r)$ is obviously to be identified with the leading term in the Glauber absorption potential. However, as was pointed out in I this potential has a spurious large-r behaviour caused by the divergence

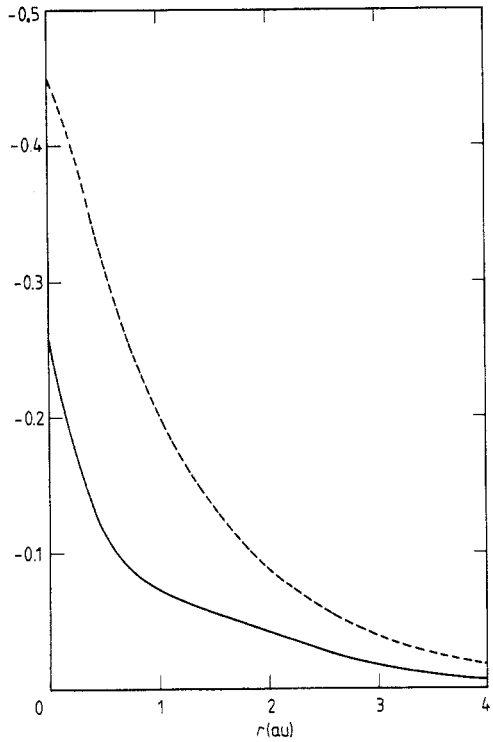

Figure 3. The quantities v_2^G (broken curve) and v_3^G (full curve) (in au) as a function of the radial coordinate r of the incident particle.

of the imaginary part of the forward Glauber amplitude, so we prefer to use the second Born absorption potential given by equations (7) and (8). We should also note that the second-order Glauber potential is purely imaginary, while the second-order Born potential has both a real and imaginary part, thereby describing, among other things, the effect of polarisation. Since the second-order Born potential does not involve an expansion in k^{-1}, it may, of course, be meaningfully employed at lower energies than the Glauber potential.

2.4. The exchange potential

Several local exchange potentials for electron–atom scattering have been proposed in recent years. In I, we used the exchange potential of Mittleman and Watson (1960),

$$V_{MW}^{\pm} = \pm\left(kp_F - \tfrac{1}{2}(k^2 - p_F^2) \ln \frac{k + p_F}{|k - p_F|} \right)(\pi k)^{-1} \tag{19}$$

where p_F is the Fermi momentum, given by

$$p_F = [6\pi \exp(-2r)]^{1/3} \tag{20}$$

in the case of electron scattering from atomic hydrogen. The superscript + denotes singlet scattering, while the superscript − denotes triplet scattering.

Another exchange potential which has been frequently used is that of Furness and McCarthy (1973) as corrected by Vanderpoorten (1975), which was derived by making

various approximations within the static-exchange model. It may be written as

$$V_{\mathrm{FM}}^{\pm} = \tfrac{1}{2}\{\tfrac{1}{2}k^2 - V_{\mathrm{st}} - [(\tfrac{1}{2}k^2 - V_{\mathrm{st}})^2 \mp 8\exp(-2r)]^{1/2}\} \tag{21}$$

in the case of an atomic hydrogen target. This potential reproduces the effect of exchange in the static exchange model rather well throughout the energy range considered in this paper, being somewhat more satisfactory in this regard than the Mittleman–Watson potential of equation (19).

Recently, however, Riley and Truhlar (1976) have proposed a modification of equation (19) in which k is replaced by a 'local momentum'

$$k_{\mathrm{L}} = (k^2 + p_{\mathrm{F}}^2)^{1/2}. \tag{22}$$

This gives us still another exchange potential,

$$V_{\mathrm{RT}}^{\pm} = \pm\left[k_{\mathrm{L}}p_{\mathrm{F}} - \tfrac{1}{2}(k_{\mathrm{L}}^2 - p_{\mathrm{F}}^2)\ln\left(\frac{k_{\mathrm{L}}+p_{\mathrm{F}}}{k_{\mathrm{L}}-p_{\mathrm{F}}}\right)\right](\pi k_{\mathrm{L}})^{-1}. \tag{23}$$

The potential $V_{\mathrm{RT}}^{\pm}$ also reproduces well the effect of exchange in the static exchange model.

All of the above exchange pseudopotentials reduce in the limit of large k to the expression

$$V_{\mathrm{Och}}^{\pm} = \pm\frac{4}{k^2}\exp(-2r) \tag{24}$$

which, when treated in first Born approximation, gives the result $\pm g_{\mathrm{Och}}$, where

$$g_{\mathrm{Och}} = -\frac{32}{k^2(K^2+4)^2} \tag{25}$$

is the familiar Ochkur (1963) expression for the elastic exchange amplitude.

Each of those potentials, however, yields different higher order exchange corrections when used in the optical model. They all give correctly the $k^{-3}K^{-2}$ large-angle correction to the imaginary part of the amplitude coming from scattering through intermediate states corresponding to the ground state of the direct and exchange channels. On the other hand, none of them gives the term of order k^{-3} in the real part of the exchange amplitude which is, in fact, the leading correction to the Ochkur approximation.

We have compared the potentials $V_{\mathrm{MW}}^{\pm}$, $V_{\mathrm{FM}}^{\pm}$ and $V_{\mathrm{RT}}^{\pm}$ by using each of them in a full optical model calculation of electron–hydrogen elastic scattering at 100 eV. The results using $V_{\mathrm{FM}}^{\pm}$ and $V_{\mathrm{RT}}^{\pm}$ agree to within about 1% over the entire range, while the potential $V_{\mathrm{MW}}^{\pm}$ gives an angular distribution which at small angles lies about 2% above and at large angles about 7% above the angular distribution obtained using $V_{\mathrm{FM}}^{\pm}$. At higher energies this discrepancy between the results using $V_{\mathrm{FM}}^{\pm}$ and those using $V_{\mathrm{MW}}^{\pm}$ diminishes rapidly. Since the statistical approach used in deriving $V_{\mathrm{MW}}^{\pm}$ seems particularly questionable in the case of atomic hydrogen, we have elected to use the Furness–McCarthy potential of equation (21) to obtain the results of the following section. However, $V_{\mathrm{RT}}^{\pm}$ would clearly have given results insignificantly different from those obtained with $V_{\mathrm{FM}}^{\pm}$.

Thus, we may write finally the singlet (+) and triplet (−) third-order optical potentials for $e^- + H$ elastic scattering as

$$V_{\mathrm{Opt}}^{\pm} = V^{(1)} + V^{(2)} + V^{(3)} + V_{\mathrm{FM}}^{\pm}. \tag{26a}$$

For $e^+ + H$ elastic scattering, the exchange potential is absent, and the third-order optical potential reads

$$V_{\text{Opt}} = V^{(1)} + V^{(2)} + V^{(3)}. \tag{26b}$$

We have used the potentials of equations (26*a*) and (26*b*) in performing the calculations presented in the next section.

3. Results and discussion

Using the third-order optical potentials given by equations (26), we have applied the method of partial waves to obtain the scattering amplitudes and differential cross sections for the elastic scattering of electrons and positrons by atomic hydrogen in the energy range 50–500 eV. Our results are summarised in tables 2–8 and in figures 4–6.

We begin in table 2 by comparing the differential cross sections for $e^- + H$ scattering at 100 eV, as obtained from several approximations to the optical potential. Taking the static potential $V^{(1)}$ as our starting point, we see that the second-order piece, $V^{(2)}$ is responsible for the largest modifications. Indeed, the addition of $V^{(2)}$ leads to a very important enhancement of the differential cross section at small angles and a reduction at larger angles. These effects have been analysed in detail in our previous work (Byron

Table 2. Comparison of various differential cross sections (in a_0^2 sr^{-1}) for electron–atomic-hydrogen scattering at 100 eV, as obtained from several approximations to the optical potential. The numbers in parentheses indicate powers of 10.

θ (deg)	Static potential $V^{(1)}$ only	Static-exchange $V^{(1)} + V_{\text{FM}}^{\pm}$	Second order without exchange $V^{(1)} + V^{(2)}$	Second order with exchange $V^{(1)} + V^{(2)} + V_{\text{FM}}^{\pm}$	Third order without exchange $V^{(1)} + V^{(2)} + V^{(3)}$	Third order with exchange $V^{(1)} + V^{(2)} + V^{(3)} + V_{\text{FM}}^{\pm}$
0	1.02	1.33	7.12	7.73	7.89	8.54
5	9.83 (−1)	1.27	3.81	4.24	4.27	4.73
10	8.73 (−1)	1.12	2.00	2.30	2.25	2.57
15	7.25 (−1)	9.19 (−1)	1.14	1.35	1.27	1.48
20	5.73 (−1)	7.14 (−1)	7.04 (−1)	8.41 (−1)	7.61 (−1)	9.02 (−1)
25	4.38 (−1)	5.36 (−1)	4.57 (−1)	5.46 (−1)	4.81 (−1)	5.71 (−1)
30	3.28 (−1)	3.94 (−1)	3.08 (−1)	3.65 (−1)	3.18 (−1)	3.75 (−1)
35	2.44 (−1)	2.87 (−1)	2.14 (−1)	2.50 (−1)	2.18 (−1)	2.53 (−1)
40	1.83 (−1)	2.11 (−1)	1.53 (−1)	1.75 (−1)	1.54 (−1)	1.77 (−1)
50	1.05 (−1)	1.17 (−1)	8.33 (−2)	9.24 (−2)	8.37 (−2)	9.29 (−2)
60	6.39 (−2)	6.91 (−1)	4.95 (−2)	5.34 (−2)	4.98 (−2)	5.37 (−2)
70	4.14 (−2)	4.37 (−2)	3.17 (−2)	3.34 (−2)	3.19 (−2)	3.36 (−2)
80	2.84 (−2)	2.95 (−2)	2.16 (−2)	2.24 (−2)	2.17 (−2)	2.25 (−2)
90	2.05 (−2)	2.10 (−2)	1.55 (−2)	1.59 (−2)	1.56 (−2)	1.60 (−2)
100	1.55 (−2)	1.57 (−2)	1.17 (−2)	1.18 (−2)	1.18 (−2)	1.19 (−2)
120	1.01 (−2)	1.00 (−2)	7.51 (−3)	7.47 (−3)	7.55 (−3)	7.51 (−3)
140	7.52 (−3)	7.39 (−3)	5.57 (−3)	5.47 (−3)	5.59 (−3)	5.50 (−3)
160	6.34 (−3)	6.19 (−3)	4.68 (−3)	4.57 (−3)	4.70 (−3)	4.59 (−3)
180	6.00 (−3)	5.85 (−3)	4.42 (−3)	4.31 (−3)	4.44 (−3)	4.33 (−3)

and Joachain 1977b) on electron scattering by helium. Both the real part $V_R^{(2)}$—which accounts for polarisation effects—and the imaginary part $V_I^{(2)}$—which describes absorption effects—lead to the enhancement of the differential cross section at small angles, while $V_I^{(2)}$ is responsible for the reduction at large angles. Looking at table 2, we see that the addition of the exchange pseudopotential also leads to an increase of the differential cross section at small angles and a decrease at large angles, but these effects are much less pronounced than for $V^{(2)}$.

Finally, the addition of the third-order potential $V^{(3)}$ is seen to lead to an increase of the differential cross section at small angles, the effect being of the order of ten per cent. At larger angles (for $\theta > 40°$ in the present case) the term $V^{(3)}$ makes no significant contribution, in agreement with our previous eikonal optical model analysis (Byron and Joachain 1974b) and with the estimates of third-order effects obtained by Vanderpoorten (1975) and by Vanderpoorten and Winters (1978). This means simply that most of the third Born term, $\bar{f}_{B3}$, is in fact generated by the potentials $V^{(1)}$ and $V^{(2)}$.

The angular distributions of the scattered electrons and positrons, as given by the present third-order optical-model theory, are presented in tables 3 and 4, respectively. In figures 4–6 we show our results at 50, 100 and 200 eV and compare them with the eikonal–Born series (EBS) results obtained by using the improved values of $\bar{f}_{B2}$ found in § 2.2, and with the experimental data of Lloyd *et al* (1974) and of Williams (1975). We have chosen to use the renormalised results of Lloyd *et al* (1974) given by van Wingerden *et al* (1977). The most striking feature of the comparisons between experiment and our third-order optical-model theory at 50, 100 and 200 eV is the fact that the average disagreement between experiment and theory is always about 25–30%, i.e. there is no significant improvement found in going from 50 to 200 eV. This is

Table 3. Differential cross section (in a_0^2 sr^{-1}) for the elastic scattering of electrons by atomic hydrogen in the energy range 50–500 eV, as obtained from the present third-order optical potential theory. The numbers in parentheses indicate powers of 10.

θ (deg)	Energy (eV)					
	50	100	200	300	400	500
0	13.0	8.54	5.65	4.51	3.88	3.47
5	9.35	4.73	2.23	1.52	1.22	1.06
10	6.26	2.57	1.14	7.91 (−1)	6.29 (−1)	5.28 (−1)
15	4.07	1.48	6.51 (−1)	4.34 (−1)	3.24 (−1)	2.54 (−1)
20	2.64	9.02 (−1)	3.85 (−1)	2.41 (−1)	1.67 (−1)	1.23 (−1)
25	1.72	5.71 (−1)	2.34 (−1)	1.36 (−1)	8.96 (−2)	6.31 (−2)
30	1.14	3.75 (−1)	1.46 (−1)	8.02 (−2)	5.05 (−2)	3.45 (−2)
35	7.75 (−1)	2.53 (−1)	9.38 (−2)	4.93 (−2)	3.01 (−2)	2.02 (−2)
40	5.37 (−1)	1.77 (−1)	6.23 (−2)	3.16 (−2)	1.89 (−2)	1.25 (−2)
50	2.78 (−1)	9.28 (−2)	3.03 (−2)	1.46 (−2)	8.51 (−3)	5.55 (−3)
60	1.59 (−1)	5.37 (−2)	1.64 (−2)	7.72 (−3)	4.44 (−3)	2.88 (−3)
70	1.00 (−1)	3.36 (−2)	9.81 (−3)	4.53 (−3)	2.59 (−3)	1.67 (−3)
80	6.82 (−2)	2.25 (−2)	6.33 (−3)	2.90 (−3)	1.65 (−3)	1.06 (−3)
90	4.98 (−2)	1.60 (−2)	4.37 (−3)	1.99 (−3)	1.13 (−3)	7.28 (−4)
100	3.83 (−2)	1.19 (−2)	3.20 (−3)	1.45 (−3)	8.23 (−4)	5.29 (−4)
120	2.56 (−2)	7.51 (−3)	1.97 (−3)	8.91 (−4)	5.05 (−4)	3.25 (−4)
140	1.96 (−2)	5.50 (−3)	1.43 (−3)	6.44 (−4)	3.65 (−4)	2.34 (−4)
160	1.67 (−2)	4.59 (−3)	1.18 (−3)	5.34 (−4)	3.02 (−4)	1.94 (−4)
180	1.59 (−2)	4.33 (−3)	1.11 (−3)	5.02 (−4)	2.84 (−4)	1.83 (−4)

Table 4. Differential cross sections (in a_0^2 sr^{-1}) for the elastic scattering of positrons by atomic hydrogen in the energy range 50–500 eV, as obtained from the present third-order optical potential theory. Numbers in parentheses are powers of 10.

θ (deg)	Energy (eV)					
	50	100	200	300	400	500
0	2.86	2.20	1.60	1.36	1.23	1.15
5	2.09	1.55	1.14	9.81 (−1)	8.96 (−1)	8.39 (−1)
10	1.44	9.66 (−1)	7.02 (−1)	5.92 (−1)	5.15 (−1)	4.53 (−1)
15	9.46 (−1)	6.17 (−1)	4.44 (−1)	3.44 (−1)	2.74 (−1)	2.22 (−1)
20	6.10 (−1)	4.14 (−1)	2.77 (−1)	1.94 (−1)	1.42 (−1)	1.08 (−1)
25	4.00 (−1)	2.85 (−1)	1.72 (−1)	1.11 (−1)	7.62 (−2)	5.53 (−2)
30	2.72 (−1)	1.99 (−1)	1.08 (−1)	6.50 (−2)	4.29 (−2)	3.02 (−2)
35	1.92 (−1)	1.41 (−1)	6.95 (−2)	3.99 (−2)	2.55 (−2)	1.77 (−2)
40	1.41 (−1)	1.01 (−1)	4.61 (−2)	2.55 (−2)	1.61 (−2)	1.10 (−2)
50	8.36 (−2)	5.42 (−2)	2.23 (−2)	1.18 (−2)	7.27 (−3)	4.90 (−3)
60	5.39 (−2)	3.14 (−2)	1.21 (−2)	6.29 (−3)	3.81 (−3)	2.55 (−3)
70	3.68 (−2)	1.96 (−2)	7.28 (−3)	3.70 (−3)	2.23 (−3)	1.49 (−3)
80	2.64 (−2)	1.31 (−2)	4.72 (−3)	2.38 (−3)	1.43 (−3)	9.48 (−4)
90	1.97 (−2)	9.22 (−3)	3.27 (−3)	1.64 (−3)	9.80 (−4)	6.50 (−4)
100	1.53 (−2)	6.86 (−3)	2.40 (−3)	1.20 (−3)	7.14 (−4)	4.73 (−4)
120	1.02 (−2)	4.32 (−3)	1.49 (−3)	7.32 (−4)	4.39 (−4)	2.90 (−4)
140	7.68 (−3)	3.17 (−3)	1.08 (−3)	5.34 (−4)	3.17 (−4)	2.10 (−4)
160	6.51 (−3)	2.65 (−3)	8.98 (−4)	4.44 (−4)	2.63 (−4)	1.74 (−4)
180	6.17 (−3)	2.50 (−3)	8.46 (−4)	4.18 (−4)	2.48 (−4)	1.64 (−4)

very surprising from a theoretical point of view. Indeed, in constructing the optical potential of equation (26*a*) we have basically used the EBS method as the foundation of our approach. Through order k^{-2} in the differential cross section the optical potential will therefore duplicate the EBS results, but it will also, of course, generate higher order corrections. If these corrections were such that they gave rise to corrections of order 30% at 50 eV, then at 200 eV, where k is down by a factor of two from its value at 50 eV, one would expect the discrepancy to be reduced by a factor of 8 or 16, depending on the angular range of the k^{-3} part of the exchange amplitude. No such reduction is seen in comparing the discrepancies between experiment and theory in the 50–200 eV range. On the other hand, at 400 eV the agreement between theory and experiment (Williams 1975) is good, although the error bars are quite a bit larger than they are at the lower energies. Finally, we note that in figures 4–6 the agreement between the third-order optical potential results and the new EBS results is excellent at small angles, precisely where we expect higher order corrections to be small because of the faster rate of convergence of the Born series at small momentum transfers.

We should also point out that even if there were a significant error in our method for determining the second-order part of the optical potential, one would still expect the resulting error in the differential cross section to decrease like k^{-2} as k increases. In this context, however, we remark that at 100 eV the difference between the EBS results for electron–hydrogen elastic scattering presented earlier (Byron and Joachain 1977c) and those evaluated using the results of this paper for $\bar{f}_{B2}$ is very small. At small angles ($\theta < 25°$), our new EBS results for the differential cross section are at most 5–6% *larger* than the old results, while at intermediate angles they are *smaller* than the old results by only as much as 5–6% (near 50°). At large angles, the difference drops to less than 1%.

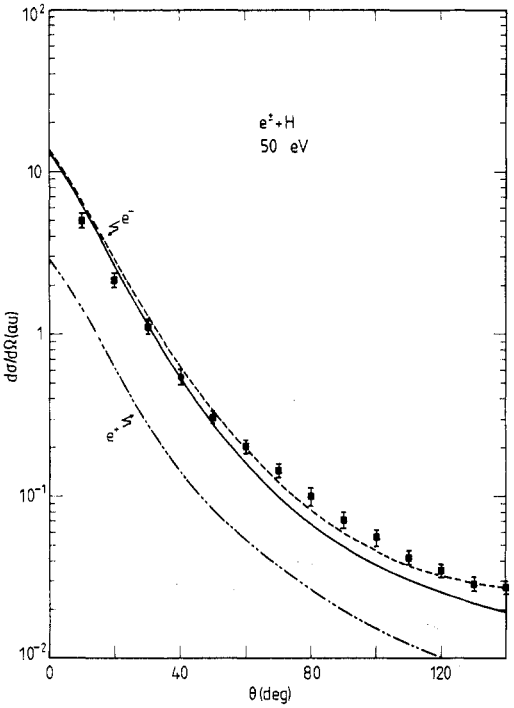

Figure 4. Differential cross section for the elastic scattering of 50 eV electrons and positrons by atomic hydrogen. The full curve is the present third-order optical potential result for electrons, the broken curve is the EBS result for electrons, and the dash–double-dot curve is the present third-order optical-potential result for positrons. The squares (■) represent the experimental data of Williams (1975) for incident electrons.

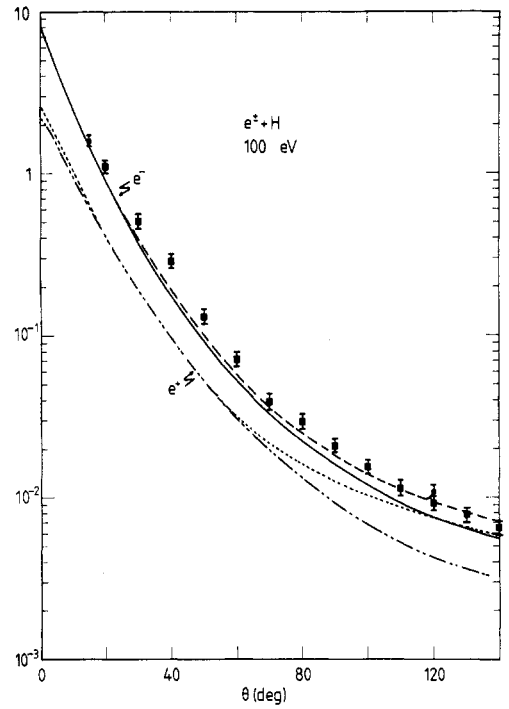

Figure 5. Same as figure 4, but at 100 eV. The squares (■) represent the experimental results of Williams (1975) for incident electrons and the dots (●) those of Lloyd *et al* (1974), renormalised by van Wingerden *et al* (1977). Also shown are the EBS results for incident positrons, represented by the dotted curve.

Thus, differences between theory and experiment are unlikely to result from inadequacies of $V^{(2)}$.

As far as $V^{(3)}$ is concerned, the situation is more complicated. In a recent paper, Yates (1979) has shown that in addition to a Glauber-like term, $\bar{f}_{G3}$, there is another term, $\bar{f}^{(2)}_{B3}$, contributing to the real part of the third Born term. This second term is formally of order k^{-2} for large k. However, it should be noted that this term vanishes (i) when the quantity $\beta = \bar{w}/k$ is set equal to zero and (ii) when the magnitude K of the momentum transfer is equal to zero. It is therefore very likely that the term $\bar{f}^{(2)}_{B3}$ is effectively of order k^{-3} or less over the entire range of momentum transfers, and thus our use of the Glauber approximation in determining $V^{(3)}$ seems justified to leading order. We therefore tentatively conclude from the present analysis that the accuracy of the experimental data needs to be improved in the energy range 50–200 eV.

Our third-order optical-potential differential cross sections for $e^+ + H$ elastic scattering, obtained by using equation (26*b*), are given in table 4 at various energies and are also plotted in figures 4–6. As noted in our previous work (Byron and Joachain 1973, Byron and Joachain 1977c), there are important differences between electron and positron scattering, particularly at small angles and (or) lower energies, where the

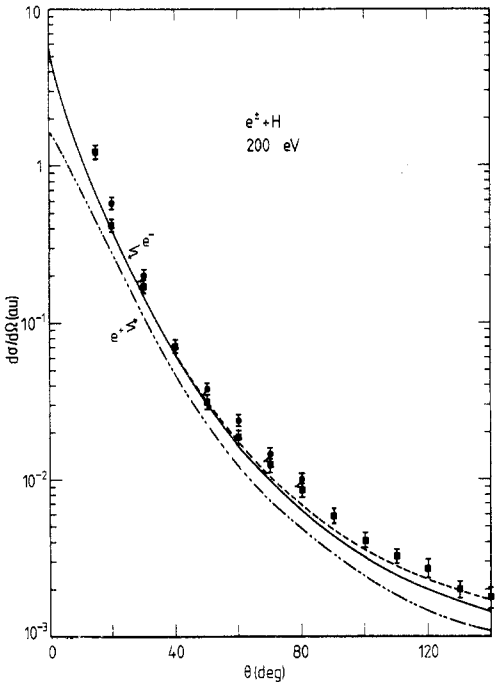

Figure 6. Same as figure 4, but at 200 eV. The squares (■) represent the experimental data of Williams (1975) for incident electrons, and the dots (●) those of Lloyd *et al* (1974), renormalised by van Wingerden *et al* (1977).

positron cross sections are much smaller than the electron ones. We recall that these differences are missing from both the first Born and the Glauber approximations which yield the same differential cross sections for positron and electron scattering. Also shown in figure 5 is the angular distribution obtained for $e^+ + H$ elastic scattering at 100 eV by using the EBS method. The EBS results are seen to agree closely with the third-order optical-potential values up to scattering angles $\theta \simeq 60°$, but at larger angles important differences appear. This is due to the fact that the static potential V_{st} is repulsive for incident positrons, so that at large momentum transfers the convergence of the Born series is even slower for incident positrons than for incident electrons.

Our total (integrated) elastic cross sections for $e^- + H$ scattering are displayed in table 5, where they are compared with the values obtained from the first Born approximation and those calculated from two other full wave treatments, namely the second-order potential method of Winters *et al* (1974) and the second-order optical potential of Vanderpoorten (1975). It is seen that our third-order optical-potential values are somewhat larger than those obtained from the second-order treatments and are in better agreement with the experimental data (Williams 1975, van Wingerden *et al* 1977), although the discrepancy with van Wingerden *et al* (1977) is still 25% at 200 eV. In table 6 we give our total complete (integrated elastic plus inelastic) cross sections for $e^- + H$ collisions and compare them with the values obtained by Winters *et al* (1974) and by Vanderpoorten (1975). The agreement between the various sets of theoretical numbers is seen to be quite good.

We now turn to the corresponding results for $e^+ + H$ scattering. In table 7, we show our total (integrated) elastic cross sections and compare them with the results of the first Born approximation and with the second-order optical potential of Vanderpoorten (1975). The agreement between the second-order treatment and the present third-order treatment is much better than that found above for total elastic $e^- + H$ scattering.

Table 5. Total elastic cross sections (in units of a_0^2) for electron scattering by atomic hydrogen.

Energy (eV)	First Born approx.	Winters *et al* (1974)	Vanderpoorten (1975)	Present third-order optical potential	Williams (1975)	van Wingerden *et al* (1977)
50	1.77	3.24†	3.08	4.16	—	—
100	9.39 (−1)	1.40	1.31	1.54	1.75‡	1.83
200	4.84 (−1)	5.81 (−1)	5.81 (−1)	6.31 (−1)	6.69 (−1)‡	7.89 (−1)
300	3.26 (−1)	—	—	3.91 (−1)	—	—
400	2.46 (−1)	—	—	2.82 (−1)	—	—
500	1.97 (−1)	—	—	2.20 (−1)	—	—

† Value obtained at 54.4 eV.
‡ Values quoted in van Wingerden *et al* (1977).

Table 6. Total cross sections (in units of a_0^2) for electron scattering by atomic hydrogen.

Energy (eV)	Winters *et al* (1974)	Vanderpoorten (1975)	Present third-order optical potential
50	12.6†	13.1	13.5
100	7.73	7.45	7.68
200	4.49	4.21	4.38
300	—	—	3.14
400	—	—	2.48
500	—	—	2.06

† Value obtained at 54.4 eV.

Table 7. Total elastic cross sections (in units of a_0^2) for positron scattering by atomic hydrogen. Numbers in parentheses are powers of 10.

Energy (eV)	First Born approx.	Vanderpoorten (1975)	Present third-order optical potential
50	1.77	1.19	1.07
100	9.39 (−1)	7.10 (−1)	7.02 (−1)
200	4.84 (−1)	4.12 (−1)	4.13 (−1)
300	3.26 (−1)	—	2.92 (−1)
400	2.46 (−1)	—	2.26 (−1)
500	1.97 (−1)	—	1.84 (−1)

In figure 7, we plot our total elastic $e^+ + H$ cross sections along with the corresponding first Born results as a function of k. This figure also includes for comparison low-energy values obtained by Winick and Reinhardt (1978) using the moment T-matrix approach. The error bars on those values result from a loss of precision involved in extrapolating from off-shell to on-shell results. It is clear that our optical-model values are tending smoothly towards the low-energy values of Winick and Reinhardt (1978). Errors resulting from the fact that only the first six partial waves are used by Winick and Reinhardt (1978) are small compared to the extrapolation errors shown in figure 7.

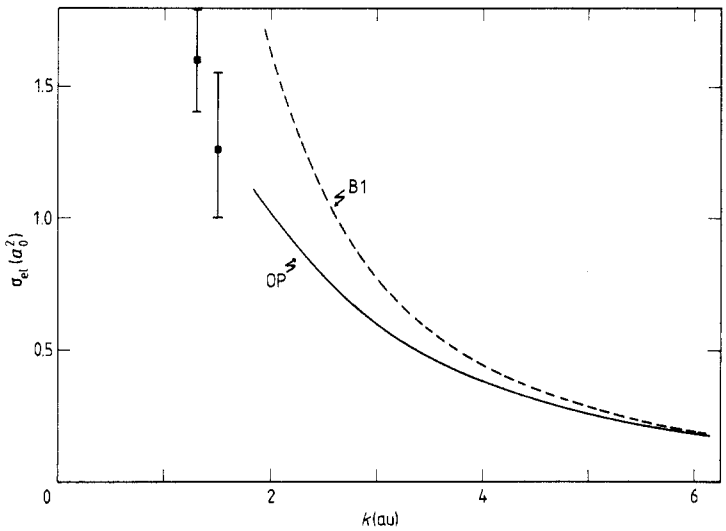

Figure 7. Total (integrated) elastic cross section for the scattering of positrons by atomic hydrogen. The full curve gives the results of the present third-order optical-potential calculation. The squares with error bars (■) are the theoretical results of Winick and Reinhardt (1978), obtained by using the moment T-matrix method. The broken curve gives the values obtained from the first Born approximation.

Finally, in table 8 we give the total complete (integrated elastic plus inelastic) cross sections for $e^+ + H$ collisions for both our third-order optical-model theory and the second-order optical-model theory of Vanderpoorten (1975). The two sets of total cross sections agree very well with each other, which shows that just as in the case of $e^- + H$ scattering the addition of the third-order potential $V^{(3)}$ has relatively little effect on total cross sections. In figure 8 we plot our total $e^+ + H$ cross sections as a function of k, with the corresponding low-energy results of Winick and Reinhardt (1978) shown for comparison. Again the error bars are associated with a loss of precision in extrapolating from off-shell to on-shell values in the Winick and Reinhardt calculation. In this case, however, there is an additional uncertainty due to the fact that partial waves with $L \geq 6$, neglected in the moment T-matrix calculation, are not expected to be negligible as they were for total elastic cross sections. Apart from the fact that the higher partial waves will increase the total cross section, it is difficult to estimate the effect of this omission. As a

Table 8. Total cross sections (in units of a_0^2) for positron scattering by atomic hydrogen.

Energy (eV)	Vanderpoorten (1975)	Present third-order optical potential
50	10.9	10.2
100	6.75	6.76
200	4.02	4.14
300	—	3.03
400	—	2.42
500	—	2.02

result, we may only deduce from figure 8 that our third-order optical-model results are certainly compatible with those obtained at low energies by Winick and Reinhardt (1978) from the moment T-matrix method.

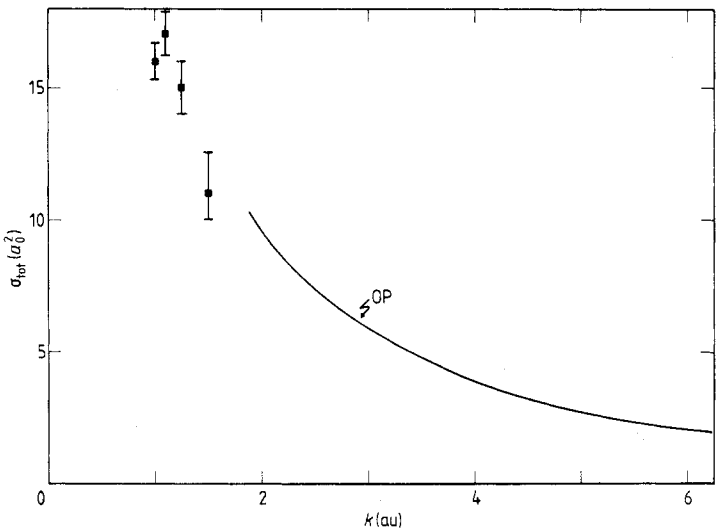

Figure 8. Total (complete) cross section for the scattering of positrons by atomic hydrogen. The full curve gives the results of the present third-order optical-potential calculation. The squares with error bars (■) are the theoretical results of Winick and Reinhardt (1978).

Acknowledgments

This work was supported in part by the NATO Scientific Affairs Division under Grant 1394 and by the US Office of Naval Research under contract N00014-78-C-0050.

Appendix

In this appendix we briefly outline the procedures used to evaluate the real part of the second Born amplitude at $\theta = 0$. Using the notation of II, we have

$$\mathrm{Re}\,\bar{f}_{B2}(K=0) = 8\pi^2 \sum_n \mathrm{P} \int \mathrm{d}\boldsymbol{q}\, \frac{\langle \boldsymbol{k}_i, 1s|V|\boldsymbol{q}, n\rangle\langle \boldsymbol{q}, n|V|\boldsymbol{k}_i, 1s\rangle}{q^2 - k^2 + 2w_{n0}} \tag{A.1}$$

where $V = Q(1/r - 1/|\boldsymbol{r} - \boldsymbol{r}_1|)$ is the electron ($Q = -1$) or positron ($Q = +1$)–hydrogen atom interaction, $w_{n0} = w_n - w_0$, P denotes the principal value and the summation on n also implies an integration over states belonging to the continuum. Defining $\boldsymbol{\Delta} = \boldsymbol{q} - \boldsymbol{k}_i$ we may write equation (A.1) as

$$\mathrm{Re}\,\bar{f}_{B2}(K=0) = \frac{2}{\pi^2} \sum_n \mathrm{P} \int \mathrm{d}\boldsymbol{q}\, \frac{|I_{1s}^n(\boldsymbol{\Delta})/\Delta^2|^2}{q^2 - k_n^2} \tag{A.2}$$

where

$$I_{1s}^{n} = \langle 1s|\exp(i\boldsymbol{\Delta}\cdot\boldsymbol{r})-1|n\rangle \tag{A.3}$$

and $k_n^2 = k^2 - 2w_{n0}$.

Let us first consider the case for which the intermediate states $|n\rangle$ are the hydrogen bound states, which we denote by $|NLM\rangle$. Writing the corresponding quantity I_{1s}^{n} as I_{1s}^{NLM}, we see from equation (A.3) that I_{1s}^{NLM} must be proportional to $Y_{LM}(\theta_\Delta, \phi_\Delta)$, where θ_Δ and ϕ_Δ are the polar angles of $\boldsymbol{\Delta}$. It is therefore convenient to define further

$$I_{1s}^{NLM}(\Delta) \equiv \left(\frac{4\pi}{2L+1}\right)^{1/2} i^L Y_{LM}(\theta_\Delta, \phi_\Delta) I_{1s}^{NL}(\Delta). \tag{A.4}$$

Using this definition, we can perform the sum on M in equation (A.2) to obtain

$$\mathrm{Re}\,\bar{f}_{B2}(K=0) = \frac{2}{\pi^2}\sum_{N,L} \mathrm{P}\int \frac{|I_{1s}^{NL}(\Delta)/\Delta^2|^2}{q^2-k_N^2} q^2 \sin\theta\, d\theta\, d\phi \tag{A.5}$$

where $k_N^2 = k^2 - 2w_{N0}$ and (θ, ϕ) are the polar angles of $\boldsymbol{q}$.

Choosing $\boldsymbol{k}_i$ to lie along the z axis, we may do the ϕ integration directly, and upon changing the integration variable from θ to Δ via $\sin\theta\, d\theta = \Delta\, d\Delta/kq$ we find

$$\mathrm{Re}\,\bar{f}_{B2}(K=0) = \frac{4}{\pi k}\sum_{N,L} \mathrm{P}\int_0^\infty dq \frac{q}{q^2-k_N^2}\int_{|q-k|}^{q+k} \Delta |I_{1s}^{NL}(\Delta)/\Delta^2|^2\, d\Delta. \tag{A.6}$$

Defining

$$g(\Delta) = \Delta |I_{1s}^{NL}(\Delta)/\Delta^2|^2 \tag{A.7}$$

and integrating by parts with respect to q in equation (A.6), we obtain finally

$$\mathrm{Re}\,\bar{f}_{B2}(K=0) = -\frac{2}{\pi k}\sum_{N,L} \mathrm{P}\int_0^\infty \ln|q^2-k_N^2|[g(q+k)-\sigma g(|q-k|)]\, dq \tag{A.8}$$

where $\sigma = \mathrm{sign}\,(q-k)$. In equation (A.8) the symbol P is a reminder to jump symmetrically over the points $q = k_N$ and $q = k$. This is of practical importance only in the case $L = 1$, where $g(\Delta)$ has a Δ^{-1} singularity.

The evaluation of equation (A.3) is straightforward for bound states $|NLM\rangle$. Using the expression of the hydrogen bound state wavefunctions in terms of the confluent hypergeometric function, one obtains readily

$$\begin{aligned} I_{1s}^{NLM}(\Delta) = {} & \frac{2\pi i^L \Delta^L Y_{LM}(\theta_\Delta, \phi_\Delta)}{N^{L+1}(2L+1)!\Gamma(L+3/2)}\left(\frac{(N+L)!}{(N-L-1)!}\right)^{1/2} \\ & \times \sum_{m=0}^{N-L-1} \frac{(L+1-N)_m \Gamma(2L+m+3)}{(2L+2)_m m!(\Delta^2+\alpha^2)^{L+2+m}}\left(\frac{2(N+1)}{N^2}\right)^{m+1} \\ & \times \sum_{\mu=0}^{\mu_{\max}} \frac{[-(m+1)/2]_\mu (-m/2)_\mu}{(L+3/2)_\mu \mu!}\left(-\frac{\Delta^2}{\alpha^2}\right)^\mu - \delta_{N1} \end{aligned} \tag{A.9}$$

where $\alpha = 1 + 1/N$ and $\mu_{\max} = m/2$ if m is even and $(m+1)/2$ if m is odd.

We now turn to the case for which the intermediate state energies lie in the continuum. We shall denote these states by $|pLM\rangle$ and the corresponding quantities I_{1s}^{n} by I_{1s}^{pLM}. Using a continuum wavefunction normalised with respect to the energy, we

obtain (with $0 \leqslant p \leqslant \infty$)

$$I_{1s}^{pLM}(\Delta) = i^L 2^{L+3} \pi^{1/2} \Big(\prod_{s=0}^{L} (p^2 s^2 + 1) \Big) \frac{Y_{LM}(\theta_\Delta, \phi_\Delta)}{(2L+1)![1-\exp(-2\pi/p)]^{1/2}} J_L \tag{A.10}$$

where

$$J_L = \int_0^\infty r^{L+2} \exp(-r) j_L(\Delta r) \exp(-ipr) {}_1F_1(L+1+i/p, 2L+2; 2ipr)\, dr. \tag{A.11}$$

We now make use of the familiar integral representation of ${}_1F_1$,

$${}_1F_1(a, b; z) = \frac{\Gamma(b)}{\Gamma(b-a)\Gamma(a)} \int_0^1 \exp(zt) t^{a-1} (1-t)^{b-a-1}\, dt \tag{A.12}$$

to perform the integral in equation (A.11). One finds

$$J_L = \frac{\Delta^L \Gamma(2L+2)\Gamma(2L+3)\pi^{1/2}}{(-4p^2)^{L+2} 2^{L+1} \Gamma(L+1+i/p)\Gamma(L+3/2)} \int_0^1 dt \frac{t^{L+i/p}(1-t)^{L-i/p}[1+ip(1-2t)]}{(t-a)^{L+2}(t-b)^{L+2}} \tag{A.13}$$

where $a = (p+\Delta-i)/2p$ and $b = (p-\Delta-i)/2p$.

The final integral on t may be performed by considering t to be a variable in the complex plane cut from $t = 0$ to $t = 1$. The integral in equation (A.13) can readily be transformed into a contour integral along straight-line segments on the top and bottom of the cut connected by small semicircles around the branch points at $t = 0$ and $t = 1$. This 'dogbone' contour may then be deformed so that it surrounds only the poles at $t = a$ and $t = b$, thus enabling one to use the familiar residue theorem. One obtains finally

$$\begin{aligned} I_{1s}^{pLM}(\Delta) = {} & \frac{(-i)^L i \Delta^L \pi^{1/2} Y_{LM}(\theta_\Delta, \phi_\Delta)}{p^3 [1-\exp(-2\pi/p)]^{1/2} \prod_{s=0}^{L} (s^2 p^2 + 1)^{1/2}} \sum_{m=0}^{L+1} \frac{(L+m+1)!}{m!} \Big(\frac{p}{\Delta} \Big)^{L+m+2} \\ & \times \sum_{\mu=0}^{L+1-m} \frac{1}{\mu!(L+1-m-\mu)!} \Big[(1+ip) \Big(\prod_{\sigma=m+\mu}^{L} (\sigma + i/p) \prod_{\tau=L+1-\mu}^{L} (\tau - i/p) \Big) \\ & \times [b^{m+\mu-1+i/p}(b-1)^{L-\mu-i/p} + (-1)^{L+m} a^{m+\mu-1+i/p}(a-1)^{L-\mu-i/p}] \\ & - 2ip \Big(\prod_{\sigma=\mu+m+1}^{L+1} (\sigma + i/p) \prod_{\tau=L+1-\mu}^{L} (\tau - i/p) \Big) [b^{m+\mu+i/p}(b-1)^{L-\mu-i/p} \\ & + (-1)^{L+m} a^{m+\mu+i/p}(a-1)^{L-\mu-i/p}] \Big]. \end{aligned} \tag{A.14}$$

In equation (A.14), $\prod_{i=m}^{n} f(i)$ denotes the usual product, with the convention that if $m > n$ the product is equal to unity.

Although this result is in closed form, the appearance of large inverse powers of Δ can cause problems of numerical precision when Δ becomes small in equation (A.14), particularly when L is large. However, for this case we can simply expand $j_L(\Delta r)$ in equation (A.11). The integral on r is then straightforward, and one obtains

$$\begin{aligned} I_{1s}^{pLM}(\Delta) = {} & \frac{i^L \Delta^L 2^{L+1} \pi^{1/2} Y_{LM}(\theta_\Delta, \phi_\Delta)}{(2L+1)!(p^2+1)^{L+1}[1-\exp(-2\pi/p)]^{1/2}} \prod_{s=0}^{L} (s^2 p^2 + 1)^{1/2} \exp(-2k^{-1} \tan^{-1} k) \\ & \times \sum_{m=0}^{\infty} (-1)^m \frac{(L+m+1)! \Delta^{2m}}{m!(1-ip)^{2m+1}} \sum_{\mu=0}^{2m+1} \frac{(L+1-i/p)_\mu (-2m-1)_\mu}{(2L+2)_\mu \mu!} \Big(\frac{2ip}{1+ip} \Big)^\mu. \end{aligned} \tag{A.15}$$

The procedure now is to use equation (A.9) in equation (A.8) to obtain for each partial wave, L, the bound-state contributions to Re $\bar{f}_{B2}(K=0)$. Only a one-dimensional numerical integration is needed. Then equations (A.14) and (A.15) are used in equation (A.8) to obtain the continuum intermediate state contribution for each L. In this case, a two-dimensional numerical integration is required. For both the continuum and bound-state cases there is no significant numerical difficulty involved.

References

Bransden B H and McDowell M R C 1977 *Phys. Rep.* **30** 207–303
—— 1978 *Phys. Rep.* **46** 249–394
Byron F W Jr and Joachain C J 1973 *Phys. Rev.* A **8** 1267–82
—— 1974a *Phys. Lett.* **49A** 306–8
—— 1974b *Phys. Rev.* A **9** 2554–68
—— 1977a *Phys. Rep.* **34** 233–324
—— 1977b *Phys. Rev.* A **15** 128–46
—— 1977c *J. Phys. B: At. Mol. Phys.* **10** 207–25
Damburg R and Karule E 1967 *Proc. Phys. Soc.* **90** 637–40
Ermolaev A M and Walters H R J 1979 *J. Phys. B: At. Mol. Phys.* **12** L779–84
—— 1980 *J. Phys. B: At. Mol. Phys.* **13** L473–8
Furness J B and McCarthy I E 1973 *J. Phys. B: At. Mol. Phys.* **6** 2280–91
Holt A R 1972 *J. Phys. B: At. Mol. Phys.* **5** L6–8
Joachain C J, Vanderpoorten R, Winters K H and Byron F W Jr 1977 *J. Phys. B: At. Mol. Phys.* **10** 227–38
Lloyd C R, Teubner P J O, Wiegold E and Lewis B R 1974 *Phys. Rev.* A **10** 175–81
Mittleman M H and Watson K M 1960 *Ann. Phys., NY* **10** 268–79
Ochkur V I 1963 *Zh. Eksp. Teor. Fiz.* **45** 734–41 (Engl. Transl. 1964 *Sov. Phys.-JETP* **18** 503–11)
Riley M E and Truhlar D G 1976 *J. Chem. Phys.* **65** 782–800
Vanderpoorten R 1975 *J. Phys. B: At. Mol. Phys.* **8** 926–39
Vanderpoorten R and Winters K H 1978 *J. Phys. B: At. Mol. Phys.* **11** 281–92
van Wingerden B, Wiegold E, de Heer F J and Nygaard K J 1977 *J. Phys. B: At. Mol. Phys.* **10** 1345–62
Williams J F 1975 *J. Phys. B: At. Mol. Phys.* **8** 2191–9
Winick J R and Reinhardt W P 1978 *Phys. Rev.* A **18** 925–34
Winters K H, Clark C D, Bransden B H and Coleman J P 1974 *J. Phys. B: At. Mol. Phys.* **7** 788–98
Yates A C 1979 *Phys. Rev.* A **19** 1550–8